

## UNIVERSITY OF TWENTE.

Faculty of Electrical Engineering, Mathematics & Computer Science

# Passive Complex-Pole Switched-Capacitor Filters

Jakub Szewczyk B.Sc. Thesis November 2019



#### Supervisors:

dr. ir. E. A. M. Klumperink B. J. Thijssen Msc dr. ir. W. Olthuis

Integrated Circuit Design (ICD)
Faculty of Electrical Engineering,
Mathematics and Computer Science
University of Twente
P.O. Box 217
7500 AE Enschede
The Netherlands

### **Abstract**

The areas concerning the reconfigurability and size reduction of filter circuits start to grow in importance in the field of wireless receivers. For this reason there is an increased interest in the capabilities of passive switched-capacitor filter architecture.

This research provides a complete analysis of the  $2^{nd}$  and  $3^{rd}$  order low-pass passive complex-pole switched-capacitor filter. The analysis gives the derivations for the filter transfer function by means of the simplified passive switched-capacitor model and verifies them by applying the "Adjoint Network" approach in LTspice simulations.

Results from the analysis show that the Q-factors for both filters are restricted to a maximum. In case of the  $2^{nd}$  order filter this is 0,7071 and for the  $3^{rd}$  order 1. Furthermore, it turns out that the filter bandwidth is reconfigurable. The comparison between the calculations and filter simulations implies that there is an increase in cut-off frequency error. This error rises from 0,4% for the  $2^{nd}$  order filter to 15% for  $3^{rd}$  order.

**Keywords:** passive switched-capacitor, switched-capacitor model, complex conjugate poles, low-pass filter, discrete time, adjoint, transfer function

## **Contents**

Αŀ	Abstract				
1	Intro	oduction	1		
2	Passive Switched-Capacitor Filter Theory				
	2.1 2.2	Difference between Active, Passive and Passive Switched-Capacitor Filters . Key operation principle of Passive Switched-Capacitor	2		
	2.3	Filters	3		
	2.4	Realization of Passive Complex-Pole Switched-Capacitor			
		Filters	6		
3	Transfer Function Calculation				
	3.1	Ideal Voltage Buffer Circuit	8		
	3.2	Ideal Voltage Inverter Circuit	9		
	3.3	Transfer Function of a $2^{nd}$ order low-pass Passive Complex-Pole Switched-			
		Capacitor Filter	10		
	3.4	Transfer Function of a $3^{rd}$ order low-pass Passive Complex-Pole Switched-Capacitor Filter	11		
4	Trar	nsfer Function Validation	14		
-	4.1	Adjoint Network Approach to obtain Frequency Response	14		
7	4.2	Verification Method for the Transfer Function	16		
		4.2.1 Method	16		
		4.2.2 LTspice: Circuits and Parameters used for verification	16		
5	Res	ults	18		
	5.1	Q-factor and cut-off frequency derivation from Transfer			
		Function	18		
	5.2	Influence of Q-factor on the Magnitude Behaviour of a Filter	20		
	5.3	Q-factor maximization vs Capacitance-ratio	21		
	5.4	Comparison between the simulations based on calculated transfer function and the Adjoint Network approach for			
		maximum achieved Q-factor	22		

Contents	iv

6	Conclusions and recommendations								
	6.1 Conclusions		24						
	6.2 Recommendations		24						
References									
Αŗ	ppendices								
A	Appendix		26						
	A.1 Code - $2^{nd}$ order lowpass Passive Complex-Pole Switched-Capacitor Filter		26						
	A 2 Code - 3 <sup>rd</sup> order lowpass Passive Complex-Pole Switched-Capacitor Filter		28						

### **Chapter 1**

## Introduction

Filters are essential building blocks of wireless receivers. They are responsible for proper frequency channel selection and provide anti-aliasing protection [1]. Future predictions for trends in the field of wireless receiver technology include the continuation in circuit size reduction and the growth in importance for filter reconfigurability (i.e multi-mode operation) [1]. Recently these trends sparked a renewed interest amongst analog circuit designers concerning the application of passive switched-capacitor filter architectures. This interest can mainly be associated with the fact that switched-capacitor filters are based on switched network structures and that they do not contain active components [2], [3]. Due to this combination, it is possible to make filters that are space saving, highly linear and possess a lower noise susceptibility [3]–[5]. Furthermore, the bandwidth of these filters can be easily reconfigured, because the cut-off frequency is set by capacitor ratios and the sampling frequency (switch clock).

Previous research [3] and [6] already discussed the possibilities of realizing these filters, mainly  $2^{nd}$  and  $3^{rd}$  order low-pass passive complex-pole switched capacitor filters, by means of the "Simplified Model" [3]. However, [3] only explains the model for the  $2^{nd}$  order filter and gives its verification. The verification was done by working out charge balance equations and comparing them to the assumed results of the filter transfer function obtained from the model. However, the actual transfer function derivation was not presented. Moreover, [6] only provides measurement results performed on the  $3^{rd}$  order filter prototype obtained by the model [3]. This thesis will focus on giving a complete overview for the transfer function derivation of the  $2^{nd}$  and  $3^{rd}$  order low-pass passive complex-pole switched capacitor filter and it will introduce another possible validation approach. In addition, the Q-factors limitations of both filters will be addressed. Chapter 2 provides the relevant filter theory. It explores the main differences between active, passive and passive switched-capacitor filters. Furthermore, it covers the simplified model used for the analysis and shows how this model can be applied to obtain complex-pole filter variant. Eventually, it presents the way they can be implemented in a real-life circuit. Chapter 3 gives a complete derivation of the transfer functions for the  $2^{nd}$  and  $3^{rd}$  order filter. Chapter 4 explains the "Adjoint Network" approach and shows how it can be applied to verify the findings of chapter 3. Chapter 5 presents the results and discusses the differences between the ones procured from simulations based on calculations and those by the method of chapter 4. Chapter 6 concludes the thesis and gives recommendations for follow-up research.

# Passive Switched-Capacitor Filter Theory

The first section of this chapter will explain the main differences between active, passive and passive switched-capacitor filters. Also, several advantages and disadvantages of passive filters will be highlighted, with respect to active ones. The second section will cover the key operation principle of passive switched-capacitor filters. The third section will introduce the simplified model for a passive switched-capacitor filter. This model makes it possible to analyze those filters in continuous time. Finally, the fourth section will discuss how passive complex-pole switched-capacitor filters can be realized.

### 2.1 Difference between Active, Passive and Passive Switched-Capacitor Filters

In general filters can be divided over two categories: passive and active filters. Passive filters are characterized by circuits that only make use of passive electric components: resistors, capacitors, inductors and switches. This means that they do not contain any amplifying elements (active components) such as: operational amplifiers, transconductors or transistors. Filters that use those components in combination with resistors and capacitors are commonly known as active filters [2], [7].

Due to the elimination of active components, passive filters in principle do not require any external power supplies in order to operate, except for the one that is feeding the circuit. In that case the power source functions as signal input. This independence on external power supplies has mainly to do with the fact that active components, which passive filters do not possess, extract power from a power source (usually a battery or voltage source) to provide more power than is available from the input signal. Essentially passive filters can never become fully de-energized, which implies that they contain memory [2].

Furthermore, it enables passive filters to have a higher voltage and current tolerance. In other words, passive filters can be used for applications which involve operations at higher voltage and current levels than active components can handle [2]. Looking from the point of view of possible noise generation, passive filters generate relatively less noise in comparison to the active ones. The noise coming from the passive filter originates from the resistive

component. That generates a thermal noise. With careful filter design the amplitude of this noise can be kept on a low level [2]. Also, because these filters are not restricted by the bandwidth limitations of the amplifying elements, they can operate well at very high frequencies [2], [7], [8]. However, there is a major drawback to passive filters. They still use inductors and resistors. In general inductors, as well as capacitors, are assumed not to dissipate any power. The reason for this is that ideally, they store energy either in electric or magnetic field without dissipation.

Overall in circuit design the use of capacitors over inductors is preferred. This preference can be deducted from the principle that capacitors tend to be smaller in size when used for applications in the low-GHz region, realistically speaking coils can not be made for frequencies lower than 1GHz. Moreover, the electrical fields of a capacitor are largely focused between the two capacitor plates, as opposed to inductors whose generated magnetic field naturally tends to extend beyond the dimensions of the core [4]. This results in capacitors being less susceptible to noise distortions originating from the receival or transmission of electromagnetic radiation from or to other components in the circuit [4]. Besides, inductors contain a lot more series resistance (caused by the winding resistance) than capacitors, which leads to additional power dissipation [9].

This is the territory where the passive switched-capacitor filters can be an attractive solution. These filters are a subgroup of passive filters that only utilize switches and capacitors. The earlier mentioned aspect in combination with the filter's switched network structure results in a circuit that saves a lot of space on a chip, does not suffer from the disadvantages of a regular passive filter, can operate at much higher sampling frequencies (confined by the resistance of the switches between charge sharing paths) and possess extremely high linearity thanks to its passive operation [3], [5]. In addition, the switched network structure causes the filter to exhibit discrete-time filter behaviour. The subject of passive switched capacitor filters will be addressed extensively in the next sections of this chapter.

## 2.2 Key operation principle of Passive Switched-Capacitor Filters

In this section a  $1^{st}$  order low-pass passive single real-pole switched-capacitor filter will be considered for the explanation of the filter's key operation principal (see figure 2.1a). Afterwards, a possible realization will be given for higher order variants of this type of filter.

The filter, as presented in figure 2.1a , is comprised of a  $g_m$ -cell, two capacitors and two switches with different activation phases ( $\phi_1$  and  $\phi_2$ ). The inclusion of the  $g_m$ -cell is strictly to acknowledge that there is a possibility of providing an additional gain to the circuit, if it would be required. The capacitors can be divided in two different categories  $C_s$  and  $C_M$ .  $C_S$  will play the role of a sampling capacitor and the other one of an integrating capacitor. In other words, the former will behave as a resistor and the latter will perform the function of a memory element [3], [6]. The switches ( $\phi_1$  and  $\phi_2$ ) will open and close during each time period  $T_S$  according to the switch clock sequence as indicated below the circuit

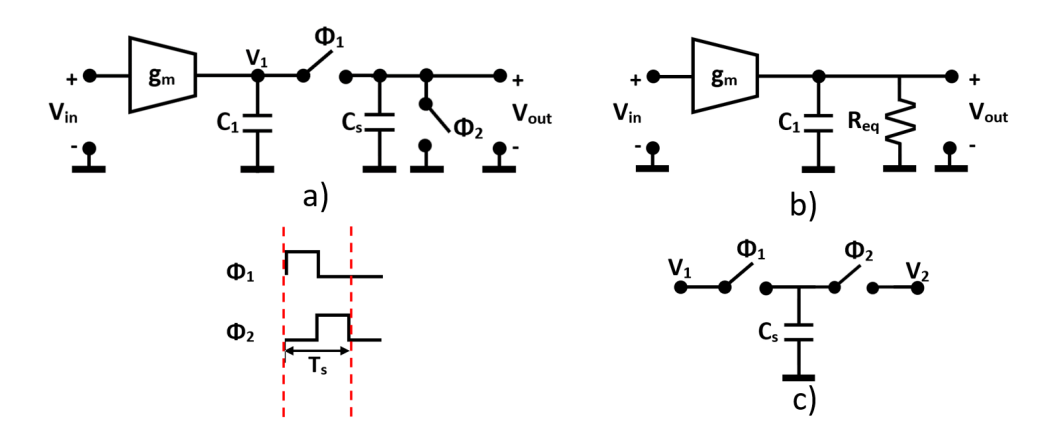


**Figure 2.1:** a)  $1^{st}$  order low-pass passive single real-pole switched-capacitor filter, with  $C_1$  being the memory capacitor  $(C_M)$  b) Figure 2.1a where the circuit (figure 2.1c) is replaced by Req, c) The switched-capacitor circuit

(see figure 2.1a). During Ts each switch is closed for a limited amount of time  $(\tau)$ , where  $\tau = \frac{Ts}{total\ amount\ of\ switches}$  assuming that all clock-phases are equal. The delay between consecutive switch clock-phases is defined as  $delay = (n-1)\tau$ , with n indicating the number of the switch (clock-phase).

When analysing how the circuit responds in time, three phases can be distinguished with each phase displaying its own specific circuit behaviour. At the initiation phase, the moment just before  $\phi_1$  is closed,  $C_M$  is charged. In phase 1, when  $\phi_1$  is closed,  $C_M$  shares its voltage with  $C_S$ . This can be thought of as  $C_S$  taking (i.e. sampling) a specific amount of charge from  $C_M$ . For this reason, we can call this filter a voltage sampling filter. In the next cycle the voltage of  $C_M$  becomes the voltage at  $C_M$  after division between  $C_M$  and  $C_S$ . Finally, in phase 2, when  $\phi_2$  closed,  $C_S$  discharges to ground. Resetting the voltage of the capacitor back to zero.

To summarize, the operations performed in phase 1 and phase 2 result in a net charge transfer ( $\Delta Q$ ) from  $V_1$  to  $V_2$ (in this case ground), this charge transfer can be represented as  $\Delta Q = C_s(V_1 - 0)$ . If the switches are flipped from  $\phi_1$  to  $\phi_2$  with a rate of  $f_S = \frac{1}{T_S}$  cycles/sec, then the charge transferred in one second can be defined as  $f_s \cdot \Delta Q = C_S f_S(V_1)$ . The term  $f_S \cdot \Delta Q$  has the units of current, because  $I = \frac{Q}{t}$ , with  $t = \frac{1}{f_S}$ . This eventually results in the formation of a resistive load  $Req = \frac{V_1}{I} = \frac{1}{f_S C_S}$ . Each new cycle, phase 1 and phase 2 are repeated. The above mentioned process eventually leads to the generation of a single real pole, since  $C_S$  is only loading  $V_{out}$  [3], [5]. The value of this pole can be determined by replacing the switched capacitor circuit (figure 2.1c) in figure 2.1a by the equivalent resistance. After this replacement figure 2.1a will now look like figure 2.1b. Using this circuit, the  $1^{st}$  order filter transfer function can be derived:

$$\left.\begin{array}{l}
I_{in} = I_{C_1} + I_{Req} \\
I_{C_1} = sC_1V_{out} \\
I_{Req} = \frac{V_{out}}{Req}
\end{array}\right\} \Rightarrow I_{in} = \frac{1 + sC_1Req}{Req}V_{out}$$
(2.1)

$$\frac{V_{out}}{I_{in}} = \frac{Req}{1 + sC_1Req} = \frac{Req}{\frac{1}{C_1Req} + s}$$
 (2.2)

From the derived denominator of equation (2.2) the value of the single real-pole (s) can be obtained,  $s=-\frac{1}{C_1Rea}$ .

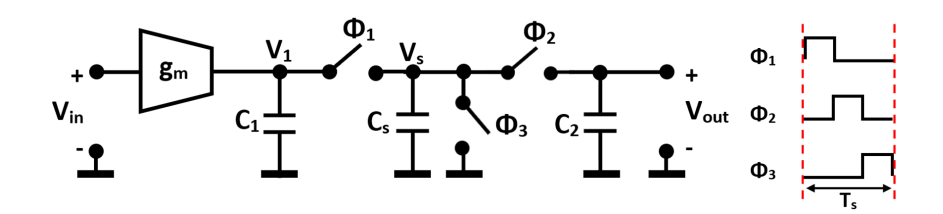


Figure 2.2: 2<sup>nd</sup> order low-pass Passive Real-Pole Switched-Capacitor Filter

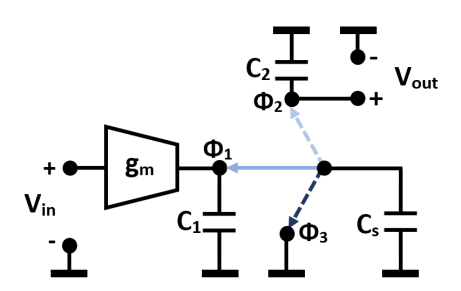
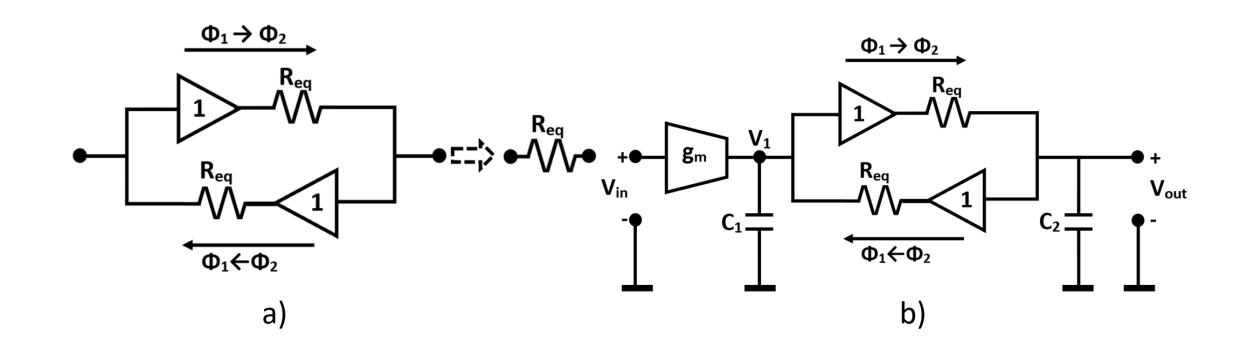


Figure 2.3: Charge rotating structure representation of figure 2.2

Now returning to the topic of realizing higher order low-pass passive real-pole switched-capacitor filters. Higher order filters can be implemented in two ways. The simplest way is by cascading two or more  $1^{st}$  (figure 2.1a) and/or  $2^{nd}$  order filters (figure 2.2). However, increasing the filter order using this approach has some serious disadvantages: first, the circuit noise will increase and linearity will deteriorate. This is caused by using transconductance/ transconductors as a link between the stages [1]. Second, the signal-to-noise ratio will decrease. This originates from the voltage loss generated by resetting the sampling capacitors at the end of each filtering stage [1], [5].

The other approach utilizes the charge rotating structure (figure 2.3). This structure does not suffer from the aforementioned weaknesses. According to Lulec, Johns and Liscidini [3] the filter order (N) equals the number of integrating capacitors ( $C_M$ ). This condition limits the amount of formed real poles to the filter order(N). Hence, Tohidian, Madadi and Staszewski [5] state that a higher order of filtering can be achieved by adding more capacitors of the same type as  $C_M$ , with inclusion of their belonging switch (clock) phases, to the circuit of figure 2.1a before ultimately discharging  $C_S$  to ground (see figure 2.2 and 2.3). In all figures,  $C_S$  is placed in the centre of the circuit. There it sequentially shares voltage with the other capacitors ( $C_{M=1}$  until  $C_{Mn}$ ) before it finally is reset, n indicates the n-th (last) integrating capacitor. This operation can be compared with the rotation of charge between  $C_S$  and the other capacitors. Therefore, the name of this structure. The output voltage is always read out at the last  $C_M$  of a given sequence.

#### 2.3 Simplified CT Model for Passive Switched-Capacitor Filters



**Figure 2.4:** a) Model of the charge/discharge flow induced by the sampling capacitor  $(C_S)$  positioned between two nodes of a switched-capacitor circuit, eventually resulting in Req, b) Continuous-time model of figure 2.2

The simplified model for passive switched-capacitor filters was introduced for the first time in [3] by Lulec, Johns and Liscidini. This model enables continuous-time analysis of a, in reality, discrete-time filter. It depends on the fundamental insight that every charge/discharge flow induced by the sampling capacitor  $(C_S)$ , positioned between two nodes of a switched-capacitor circuit (figure 2.1c), can be modelled by an ideal voltage buffer in series with equivalent resistance (Req) (figure 2.4a). The Req models the amount of charge flow. As shown in the previous section, the value of Req is equivalent to  $\frac{1}{f_sC_s}$ , with  $f_S$  being the sampling frequency and  $C_S$  the capacitance of the sampling capacitor. The function of ideal buffers in this model is to ensure the unilateral flow of the charge. When the model is applied to switched capacitor circuit as shown in figure 2.2, the obtained continuous-time circuit will then look like figure 2.4b.

## 2.4 Realization of Passive Complex-Pole Switched-Capacitor Filters

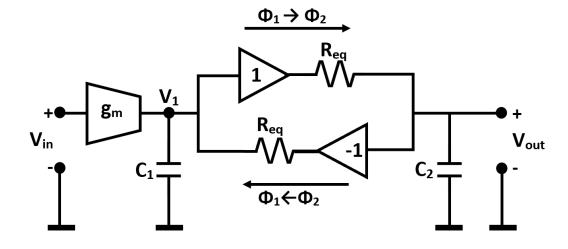


Figure 2.5: The circuit of figure 2.4b with the gain in the feedback loop replaced by -1

Before continuing with how passive complex-pole switched-capacitor filters are realized, let us first take a step back to explain why it is beneficial to have complex instead of real pole filters. The main reason for this is that complex poles always manifest themselves in conjugate pairs [10]. This leads to a sharper filter frequency responds, and it provides better frequency selectivity [1].

Normally complex-pole realization comes paired with the use of active components in order to construct feedback loops, which enable the real poles to be moved into the complex plane [1], [3]. However, thanks to the circuit obtained in figure 2.4b it is possible to transform the created real-poles into the complex-conjugate variant by simply interchanging the ideal voltage buffer in the feedback loop to an ideal voltage inverter (voltage controlled voltage source with gain of -1) [3]. The circuit will now resemble figure 2.5. The network represented in this figure is nonreciprocal, because of the unidirectional operation of the buffer and inverter. The inversion of gain in the feedback loop allows the formation of complex-poles using passive components [3].

Although, how can the inverting feedback loop be implemented in an electric circuit? The most straightforward is by cross-coupling the positive and negative terminals between the sampling capacitor  $C_S$  and the other  $C_M$  capacitors and using a differential circuit structure [3].

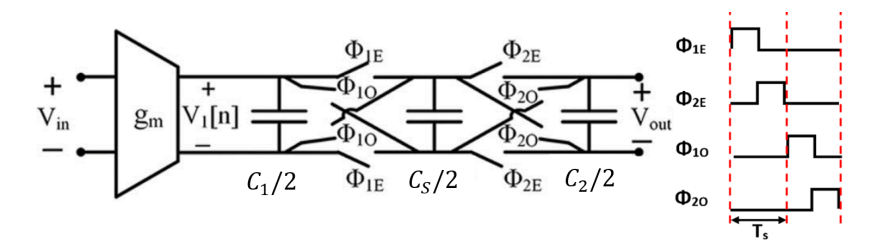


Figure 2.6: Differential representation of figure 2.5 [3]

After the implementation of the cross-coupling, figure 2.5 will be transformed into figure 2.6. In this figure the switch clock phases  $\phi_1$  and  $\phi_2$  are subdivided into even and odd clock phases ( $\phi_{1E}$ ,  $\phi_{2E}$ ,  $\phi_{1O}$  and  $\phi_{2O}$ ). During the even clock phases the circuit in figure 2.6 will respond in the same way as the one in figure 2.2, while during the odd phases the charge inversion operation will be ensured [3]. Nonetheless, still a remark needs to be made in regard to the capacitance values of all capacitors. Due to the differential structure each of the original capacitors( $C_1$ ,  $C_2$  and  $C_S$ , from now on referred to  $C_{1[Original]}$ ,  $C_{2[Original]}$  and  $C_{S[Original]}$  ) in figure 2.5 can be regarded as two capacitors in parallel, one indicating the charge moment at the even phases ( $C_{1[E]}$ ,  $C_{2[E]}$  and  $C_{S[E]}$ ) and the other at the odd ones( $C_{1[O]}$ ,  $C_{2[O]}$  and  $C_{S[O]}$ ). Based on this, one can derive the following relation between the capacitors:

$$C_{1[Original]} = C_{1[E]} + C_{1[O]}$$

$$C_{1[E]} = C_{1[O]} = C_{1}$$

$$C_{1[Original]} = 2C_{1} \Rightarrow C_{1} = \frac{C_{1[Original]}}{2}$$
(2.3)

The presented relation also holds for  $C_2$  as well as  $C_S$ . This explains why the values of each capacitor in figure 2.6 are half of those in figure 2.2.

## **Chapter 3**

## **Transfer Function Calculation**

The first two sections of this chapter will give the characteristics and internal schematics of an ideal op-amp voltage buffer and inverter. In this thesis the earlier mentioned op-amp implementations of the ideal (inverting) buffers will be used to analyze the filter circuits. These circuits were obtained from the simplified model that was introduced in the chapter 2. The third section will give the derivation of the  $2^{nd}$  order filter's transfer function. The fourth section will have the same purpose as the third, though it will discuss the case of the  $3^{rd}$  order filter.

#### 3.1 Ideal Voltage Buffer Circuit

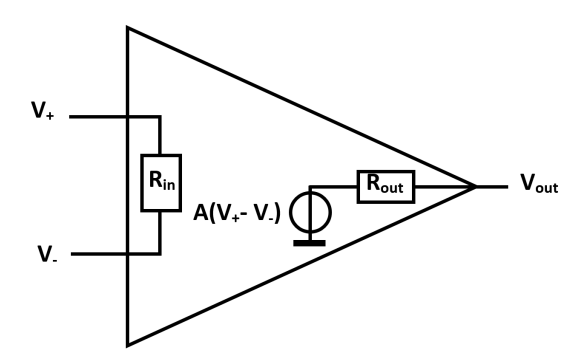
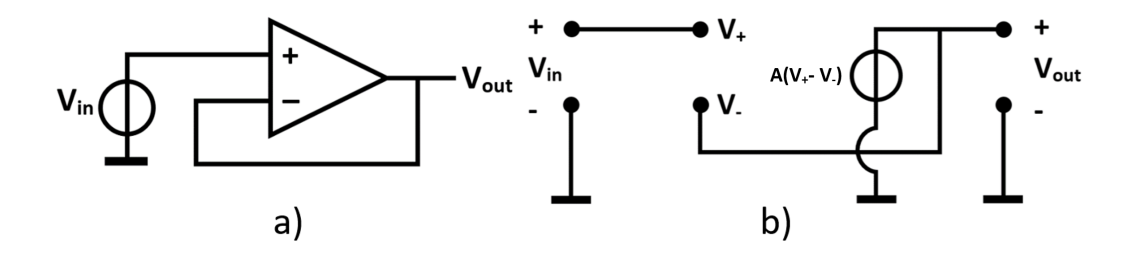


Figure 3.1: Schematic of an ideal op-amp

An ideal voltage buffer can be realized with a voltage follower circuit, as depicted in figure 3.2a. This circuit contains an ideal op-amp (figure 3.1), which has the following parameters [11]:

- $V_{out} = A(V_+ V_-)$ , with A indicating the amplifier gain. For an Ideal op-amp this gain is  $\infty$ .
- $R_{in} = \infty \Omega$
- $R_{out} = 0 \Omega$



**Figure 3.2:** Schematic of the Ideal Buffer, a) Op-amp schematic drawn without internal components displayed, b) Op-amp schematic drawn with internal components

Based on the ideal buffer presented in figure 3.2b, the relation between  $V_{in}$  and  $V_{out}$  equals:

$$\begin{cases}
V_{out} = A(V_{+} - V_{-}) \\
V_{+} = V_{in} \\
V_{-} = V_{out}
\end{cases} \Rightarrow V_{out} = \frac{A}{1 + A}V_{in}$$
(3.1)

Because  $A = \infty$ , equation (3.1) can be simplified to  $V_{out} = V_{in}$ .

### 3.2 Ideal Voltage Inverter Circuit

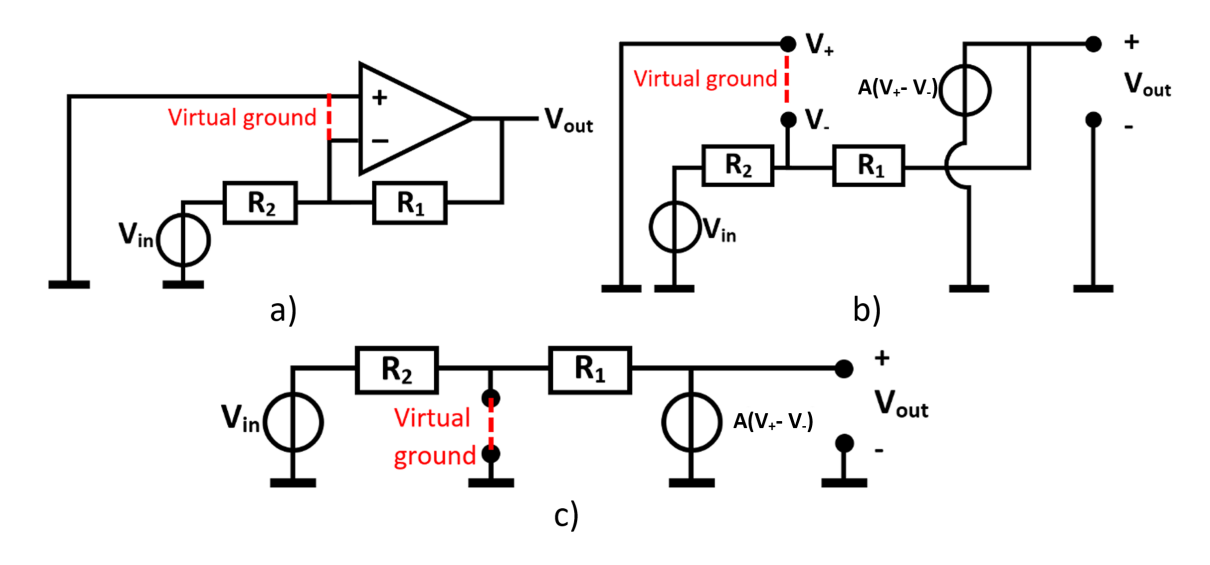


**Figure 3.3:** Schematic of the Ideal Inverter, a) Op-amp schematic drawn without displayed internal components, b) Op-amp schematic drawn with internal components, c) Simplified schematic of figure 3.3b

The ideal voltage inverter can be realized using the circuit presented in figure 3.3a. This figure can be redrawn into figure 3.3b after replacing the ideal op-amp with its internal components (figure 3.1) and applying its parameters as specified in the section 3.1 [11].

Furthermore, one can speak of a virtual ground connection, because:

$$V_{out} = A(V_{+} - V_{-})$$
 
$$V_{+} - V_{-} = \frac{V_{out}}{A} = 0 \quad (A = \infty)$$
 (3.2)

Due to the presence of a virtual ground figure 3.3b can be further simplified into figure 3.3c. From figure 3.3c it is possible to obtain the relation between  $V_{in}$  and  $V_{out}$ . Assuming  $R_1$  equals  $R_2$ , this relation turns out to be:

$$V_{out} = -\frac{R_1}{R_2} V_{in} = -V_{in} {(3.3)}$$

## 3.3 Transfer Function of a $2^{nd}$ order low-pass Passive Complex-Pole Switched-Capacitor Filter

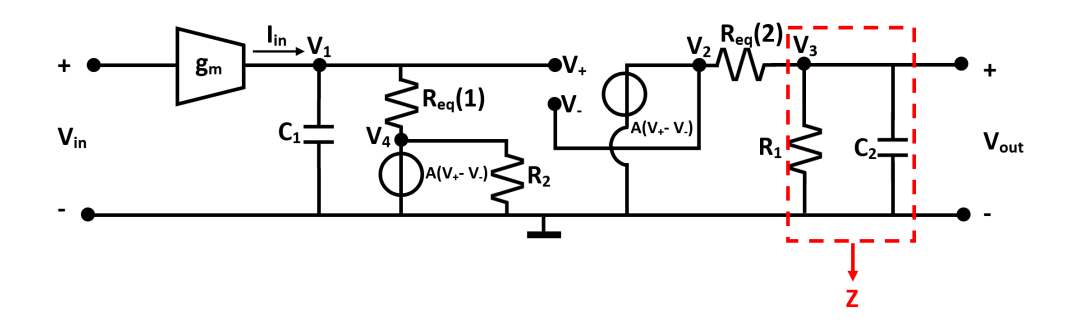


**Figure 3.4:**  $2^{nd}$  order low-pass Passive Complex-Pole Switched-Capacitor filter, figure 2.5 after replacing the ideal buffers and inverter by figure 3.2b and 3.3c

The simplified model of a  $2^{nd}$  order filter is presented in figure 2.5 and 3.4. To derive the transfer function of this filter, figure 3.4 will be used. Based on this figure the following equations can be derived:

#### **Buffer equations:**

$$V_2 = V_1$$
 (3.4)

#### Inverter equations:

$$\begin{vmatrix}
V_4 = -V_3 \\
V_3 = V_{out}
\end{vmatrix} \Rightarrow V_4 = -V_{out}$$
(3.5)

#### Impedance (Z):

$$Z = \frac{1}{sC_2} /\!\!/ R_1$$

$$= \frac{R_1}{1 + sC_2 R_1}$$
(3.6)

Assuming  $R_1 >> 1$  the impedance will be:

$$Z = \frac{1}{sC_2} \tag{3.7}$$

KCL on node  $V_1$  gives:

$$-I_{in} + I_{C_1} + I_{Req}(1) = 0$$

$$I_{in} = I_{C_1} + I_{Req}(1)$$
(3.8)

$$\left.\begin{array}{c}
I_{C_{1}} = V_{C_{1}} \cdot sC_{1} \\
V_{C_{1}} = V_{1} - 0 = V_{1} \\
I_{Req}(1) = \frac{V_{1} - V_{4}}{Req} = \frac{V_{1} + V_{out}}{Req}
\end{array}\right\} \Rightarrow I_{in} = \frac{(1 + sC_{1}Req)V_{1}}{Req} + \frac{V_{out}}{Req}$$
(3.9)

$$\begin{cases} V_{out} = Z \cdot I_{Req}(2) \\ = \frac{1}{sC_2} \cdot I_{Req}(2) \end{cases} \Rightarrow I_{Req}(2) = sC_2V_{out} \\ I_{Req}(2) = \frac{V_2 - V_{out}}{Req} \Rightarrow V_1 = V_2 = I_{Req}(2)Req + V_{out} \end{cases} \Rightarrow V_1 = (sC_2Req + 1)V_{out}$$
 (3.10)

The substitution of equation (3.10) into (3.9) gives:

$$I_{in} = \frac{(1 + sC_1Req)(1 + sC_2Req) + 1}{Req}V_{out}$$
(3.11)

Finally resulting in the transfer function of the  $2^{nd}$  order filter (TF):

$$TF = \frac{V_{out}}{I_{in}}$$

$$= \frac{Req}{(1+sC_1Req)(1+sC_2Req)+1}$$

$$= \frac{Req}{s^2C_1C_2Req^2+s(C_1+C_2)Req+2}$$
(3.12)

## 3.4 Transfer Function of a $3^{rd}$ order low-pass Passive Complex-Pole Switched-Capacitor Filter

The simplified model of a  $3^{rd}$  order filter is presented in figure 3.5b and figure 3.6. To derive the transfer function of this filter, figure 3.6 will be used. Based on this figure the following equations can be derived:

#### **Buffer equations:**

$$V_1 = V_2 V_3 = V_4$$
 (3.13)

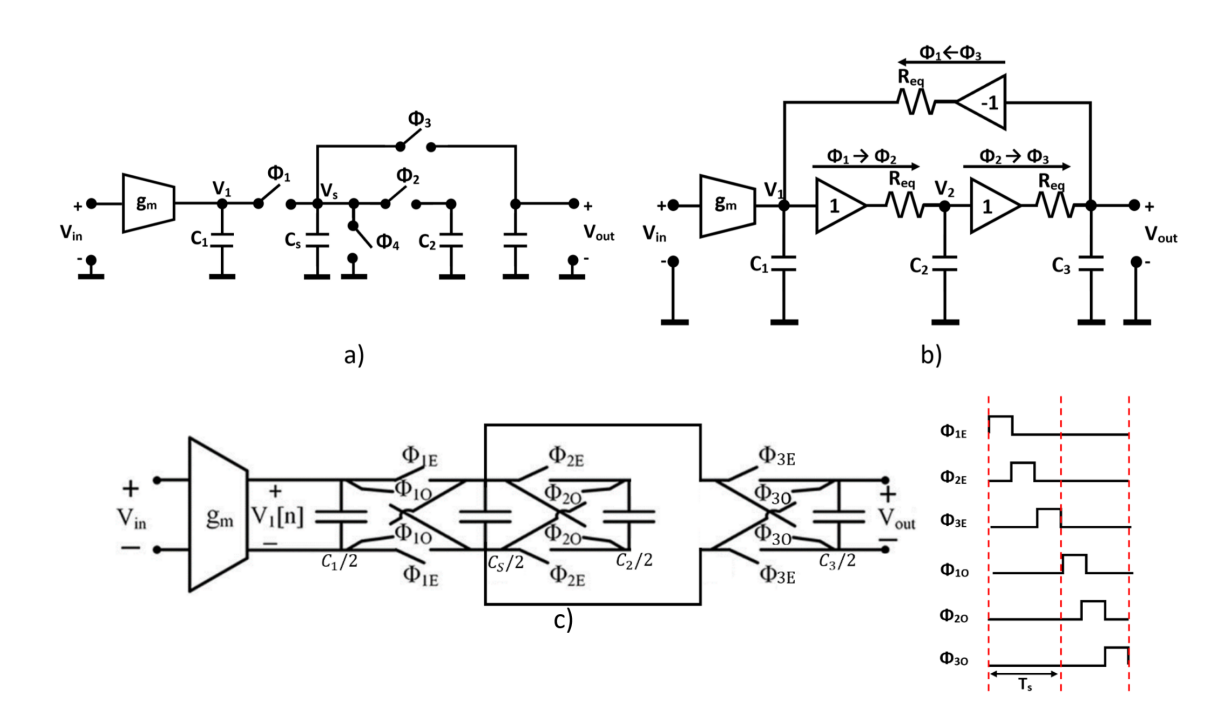


**Figure 3.5:** a)  $3^{rd}$  order low-pass Passive Complex-Pole Switched-Capacitor filter, b) Simplified Model of 3.5a, c) Differential representation of figure 3.5b

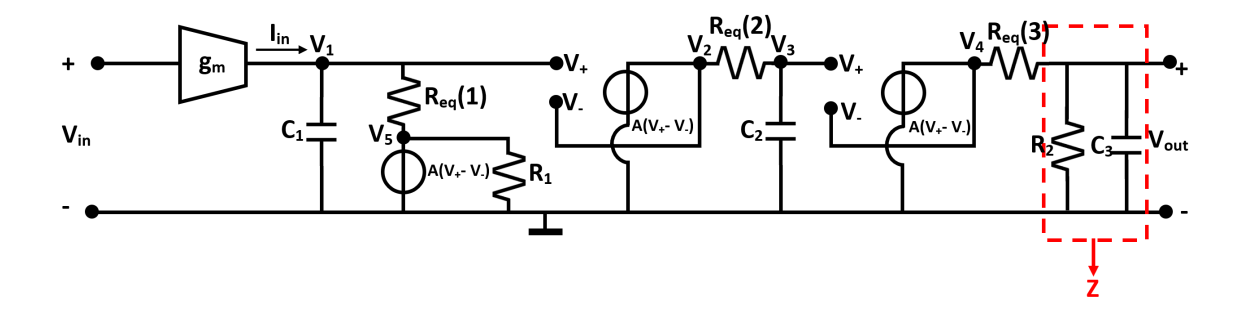


Figure 3.6: Figure 3.5b after replacing the ideal buffers and inverter by figure 3.2b and 3.3c

#### Inverter equations:

$$V_5 = -V_{out} \tag{3.14}$$

#### Impedance (Z):

$$Z = \frac{1}{sC_3} /\!\!/ R_2$$

$$= \frac{R_2}{1 + sC_3 R_2}$$
(3.15)

Assuming  $R_2 >> 1$  the impedance will be:

$$Z = \frac{1}{sC_3} {(3.16)}$$

KCL on node  $V_1$  gives:

$$-I_{in} + I_{C1} + I_{Req}(1) = 0$$

$$I_{in} = I_{C1} + I_{Req}(1)$$
(3.17)

$$\left. \begin{array}{l}
I_{C1} = V_{C1} \cdot sC_1 \\
V_{C1} = V_1 - 0 = V_1 = V_2 \\
I_{Req}(1) = \frac{V_1 - V_5}{Req} = \frac{V_2 + V_{out}}{Req}
\end{array} \right\} \Rightarrow I_{in} = \frac{(1 + sC_1Req)V_2}{Req} + \frac{Vout}{Req} \tag{3.18}$$

$$\frac{I_{C2} = V_{C2} \cdot sC_2}{V_{C2} = (V_3 - 0)} \} \Rightarrow I_{C2} = sC_2V_3$$
 (3.19)

$$\left\{ I_{Req}(2) = I_{C2} \atop I_{Req}(2) = \frac{V_2 - V_3}{Req} \right\} \Rightarrow I_{C2} = \frac{V_2 - V_3}{Req} \\
 \left\{ I_{C2} = sC_2V_3 \right\} \Rightarrow V_2 = (1 + sC_2Req)V_3 \\
 = (1 + sC_2Req)V_4$$
(3.20)

$$\begin{cases} V_{out} = Z \cdot I_{Req}(3) \\ = \frac{1}{sC_3} \cdot I_{Req}(3) \end{cases} \Rightarrow I_{Req}(3) = sC_3V_{out}$$

$$I_{Req}(3) = \frac{V_4 - V_{out}}{Req} \Rightarrow V_4 = I_{Req}(3)Req + V_{out}$$

$$\Rightarrow V_4 = (sC_3Req + 1)V_{out}$$

$$(3.21)$$

After filling in equation (3.21) into equation (3.20) the expression for  $V_2$  is obtained:

$$V_2 = (1 + sC_2Req)(1 + sC_3Req)V_{out}$$
(3.22)

The substitution of equation (3.22) into equation (3.18) gives:

$$I_{in} = \frac{(1 + sC_1Req)(1 + sC_2Req)(1 + sC_3Req) + 1}{Req}V_{out}$$
(3.23)

Finally resulting in the transfer function of the  $3^{rd}$  order filter (TF):

$$TF = \frac{V_{out}}{I_{in}}$$

$$= \frac{Req}{(1+sC_1Req)(1+sC_2Req)(1+sC_3Req)+1}$$

$$= \frac{Req}{s^3C_1C_2C_3Req^3+s^2(C_1C_2+C_1C_3+C_2C_3)Req^2+s(C_1+C_2+C_3)Req+2}$$
(3.24)

## **Chapter 4**

## **Transfer Function Validation**

This chapter introduces the concept of the "Adjoint Network" approach. In section 4.2 this approach will be used for the verification of the transfer functions derived in chapter 3.

#### 4.1 Adjoint Network Approach to obtain Frequency Response

The "Adjoint Network" approach is centered around the findings presented in the publication by Pavan and Klumperink [12]. In this publication was proven that the output samples of a linear periodically time-varying (LPTV) system (for example a switched-capacitor network) that varies with a frequency  $f_S$ , that is driven by an input signal x(t) and whose output is as well sampled at  $f_S$  can be approximated by the output samples obtained from a linear time-invariant (LTI) filter that is driven by x(t) and is sampled at the output at a rate  $f_S$ . In addition, the impulse response (heq(t)) of the equivalent LTI system can then be obtained using the adjoint of the LPTV network [12].

One can find heq(t) as follows. The original LPTV network(N) needs to be redrawn to its adjoint( $\widehat{N}$ ) (for reference see figure 4.1a and b). This can be done by applying the following transformations [12]:

- 1. Every linear resistor, capacitor and inductor in the original network remains unchanged in the adjoint.
- 2. The switches controlled by a clock  $\phi(t)$  will in the adjoint be operated by its "time-reversed" version  $\phi(-t)$ .
- 3. Every controlled source will be replace by its equivalent adjoint version as is indicated in figure 4.2.

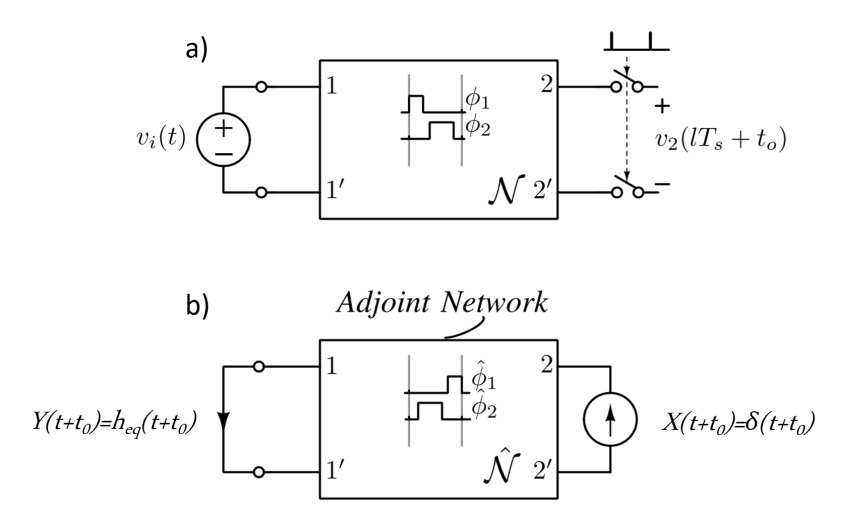


Figure 4.1: a) An LPTV network [12], b) Equivalent adjoint LTI filter of figure 4.1a [12]

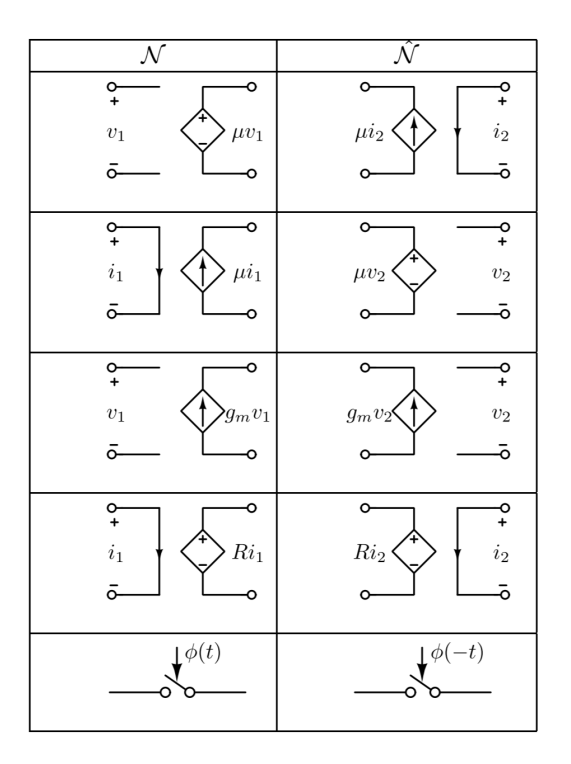


Figure 4.2: Transformations of Linear Controlled Sources and Periodically Operated Switches from N to  $\widehat{N}$  [12]

From figure 4.1b one can conclude that the output current at a time instance  $t+t_0$  can be described by a convolution of  $x(t+t_0)$  with the network's equivalent impulse response  $heq(t+t_0)$ , because of

$$y(t+t_0) = \int_{-\infty}^{\infty} x(\tau)heq((t+t_0) - \tau)d\tau$$
 (4.1)

When the input current  $x(t+t_0)$  is set to the Dirac delta function response, then the output

current  $y(t+t_0)$  results in

$$y(t+t_0) = \int_{-\infty}^{\infty} \delta(\tau) heq((t+t_0) - \tau) d\tau = heq(t+t_0)$$
(4.2)

The frequency response can now be derived from the Fourier-transform of  $heq(t + t_0)$ .

#### 4.2 Verification Method for the Transfer Function

#### 4.2.1 Method

The transfer function verification will be performed in three steps. In the first step Matlab will generate magnitude plots for the transfer functions obtained in chapter 3 at maximum Q-factor (code displayed in Appendix A.1 and A.2). The maximum Q-factor calculations for the  $2^{nd}$  and  $3^{rd}$  order low-pass passive complex-pole switched-capacitor filter are presented in the next chapter "Results". Section 5.1 presents the equations and 5.3 the calculation results.

The second step will apply the "Adjoint Network" approach introduced in the previous section on the filter circuits from section 2.4 (figure 2.6) and 3.4 (figure 3.5c), giving rise to circuits that are suitable for LTspice simulation. The circuit that were presented in section 2.4 and 3.4 cannot be used in LTspice due to the fact that LTspice can only perform AC simulations in continuous and not discrete time. For the new circuits the reader is referred to figure 4.3 in case of  $2^{nd}$  order filter and to figure 4.4 for the  $3^{rd}$  order filter. The magnitude plot, which normally can be obtained from the Bode plot in AC simulation, is now obtained using transient simulation. As was explained in the previous section, the transfer function (Heq(f)) can then be found by taking the FFT (Fast Fourier Transform) of the output current (heq(t)), which as well is the impulse response of a given filter.

Eventually, in the third step a comparison will be made between the results obtained from the Matlab and LTspice simulation. The comparison will pay attention to the values of the cut-off frequency and attenuation in the stopband. These parameters should be equal for both simulation types and match the filter theory. The theory implies that the  $2^{nd}$  order filters should have stopband attenuation of 40dB/decade and  $3^{rd}$  order filter 60 dB/decade.

#### 4.2.2 LTspice: Circuits and Parameters used for verification

The parameters used for the LTspice simulation of the adjoint  $2^{nd}$  as well as  $3^{rd}$  order low-pass passive complex-pole switched capacitor filters can be found in table 4.1. The simulations were performed at a sampling frequency  $(f_S)$  of 160MHz. The capacitors  $(C_1$  until  $C_3$ ), with the exception of  $C_S$  (200fF), were equally valued for both filters and set to 10pF. It is important to notice that one should pay attention to the capacitor definitions in figure 4.3 and 4.4, while the earlier stated capacitors  $(C_1, C_2, C_3 \text{ and } C_S)$  are used in their definitions. Furthermore, to make sure that the switch clock phases do not overlap each other, it was chosen to set the time that a switch is active (Ton) to  $\Gamma(=\frac{T_S}{number\ of\ switches\ in\ the\ even\ or\ odd\ phase})$  minus four times the rise time (Trise).

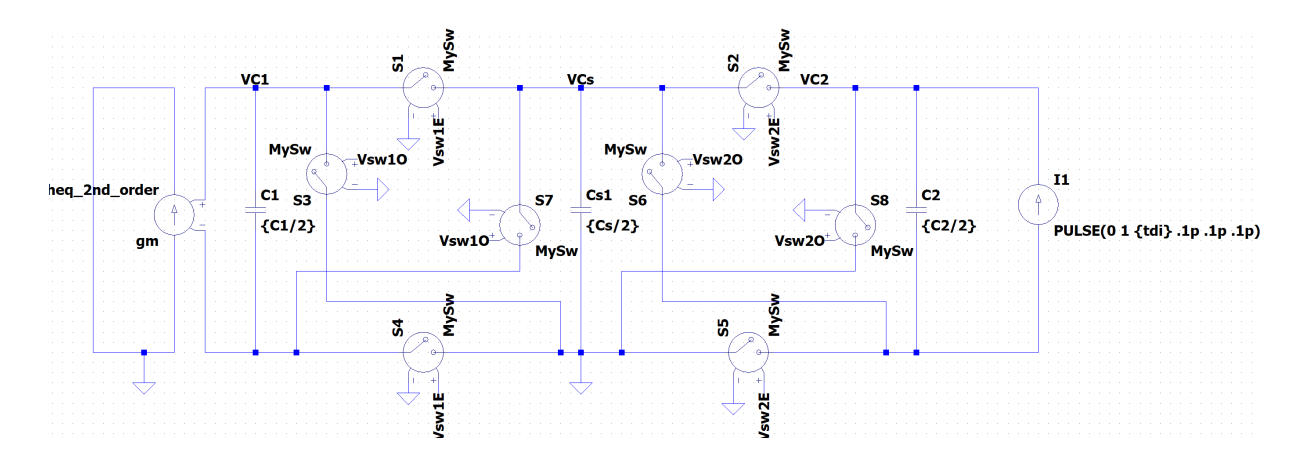


Figure 4.3: Adjoint version of figure 2.6

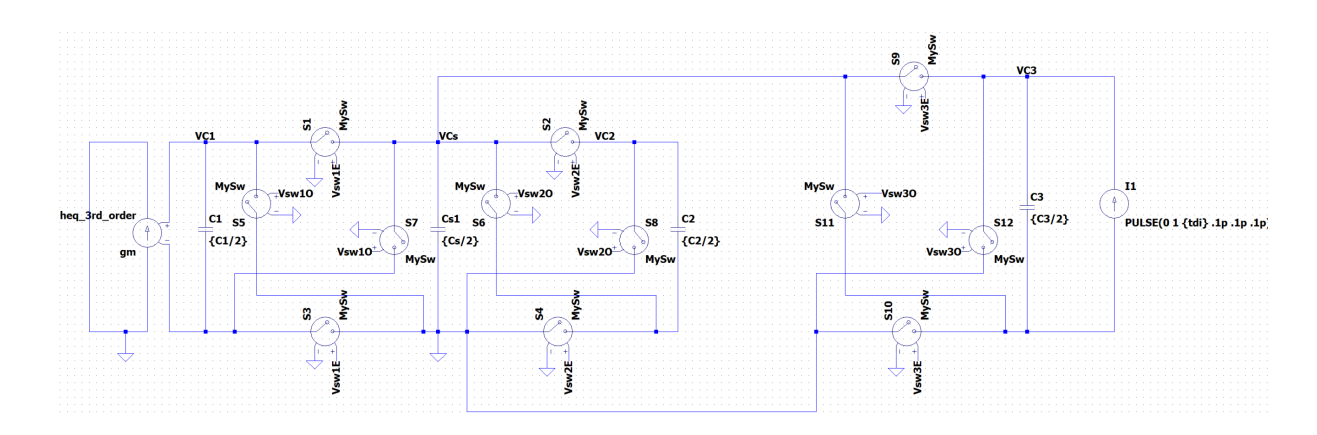


Figure 4.4: Adjoint version of figure 3.5c

**Table 4.1:** LTspice Simulation parameters for the  $2^{nd}$  and  $3^{rd}$  order low-pass Passive Complex-Pole Switched-Capacitor Filter

LTspice Simulation Parameters									
Switch-initiation	$2^{nd}$ order	$3^{rd}$ order	Switch	Tdelay $2^{nd}$	Tdelay $3^{rd}$				
Parameters			Phase	order	order				
Vinitial	0V	0V	Vsw3O	_	0				
Von	1V	1V	Vsw2O	0	$\frac{T_S}{3}$				
Trise	1ps	1ps	Vsw1O	$\frac{T_S}{2}$	$\frac{T_S}{3}$ $\frac{2T_S}{3}$				
Tfall	1ps	1ps	Vsw3E	_	$T_S$				
Ton	$\frac{T_S}{2} - 4Trise$	$\frac{T_S}{3} - 4Trise$	Vsw2E	$\parallel T_S$	$\frac{4T_S}{3}$				
Tperiod	$2 \cdot T_S$	$2 \cdot T_S$	Vsw1E	$\frac{3T_S}{2}$	$\frac{4T_S}{3}$ $\frac{5T_S}{3}$				

### **Chapter 5**

## Results

The results presented in this chapter were obtained from Matlab and LTspice simulations. Matlab (Appendix A.1 and A.2) was used to implement the transfer functions (derived in chapter 3) and to calculate the maximum achievable Q-factor with the belonging filter cut-off frequency. The definitions of Q-factor and cut-off frequency, that were used in the simulations, are formulated in section 5.1. For the verification of the Matlab results, LTspice was applied. The LTspice simulations were based on the "Adjoint Network" model. The model and the parameters of these simulations were discussed in chapter 4. All simulations were performed at a sampling frequency  $(f_S)$  of 160MHz.

## 5.1 Q-factor and cut-off frequency derivation from Transfer Function.

In order to obtain the Q-factor and the cut-off frequency, the  $2^{nd}$  order filter transfer function given in section 3.3 equation (3.12) needs to be rewritten to the standard  $2^{nd}$  order biquad filter formula. The standard formula is defined as follows [2]:

$$TF = \frac{{\omega_0}^2}{s^2 + \frac{{\omega_0}}{O}s + {\omega_0}^2} \tag{5.1}$$

Rearranging the terms in equation (3.12) to the standard formula results in:

$$TF = \frac{Req}{2} \cdot \frac{\frac{2}{C_1 C_2 Req^2}}{s^2 + \frac{\sqrt{2}}{\sqrt{C_1 C_2 Req}} \cdot \frac{C_1 + C_2}{\sqrt{2C_1 C_2}} s + \frac{2}{C_1 C_2 Req^2}}$$
(5.2)

$$\omega_0^2 = \frac{2}{C_1 C_2 Req^2} \Rightarrow \omega_0 = \sqrt{\frac{2}{C_1 C_2 Req^2}} = \frac{\sqrt{2}}{\sqrt{C_1 C_2 Req}}$$
 (5.3)

$$f_{cut-off} = \frac{\omega_0}{2\pi} = \frac{1}{\pi\sqrt{2C_1C_2}Req}$$
 (5.4)

$$\frac{1}{Q} = \frac{C_1 + C_2}{\sqrt{2C_1C_2}} \Rightarrow Q = \frac{\sqrt{2C_1C_2}}{C_1 + C_2}$$
(5.5)

The same can be done for the  $3^{rd}$  order filter transfer of section 3.4 equation (3.24).

At first the denominator of equation (3.24) needs to be rewritten in terms that represent  $1^{st}$  and  $2^{nd}$  order filter behaviour.

$$TF = \frac{Req}{(ds+1)(as^2+bs+c)} = \frac{Req}{ads^3 + (a+bd)s^2 + (b+cd)s + c}$$
 (5.6)

Since it is know that complex-poles only appear in conjugate pairs [10] and that the order of a passive complex-pole switched capacitor filter indicates the number of formed poles [3], it can be deduced that the  $3^{rd}$  order filter can realize two complex-poles and one real-pole. This implies that the value of variable d can be determined by finding the single realized real-pole. For example, this can be done by applying the root function of Matlab on the denominator of equation (3.24), under the condition that the values of  $C_1, C_2$  as well as  $C_3$  are set to 10pF and  $C_s$  to 200fF. This results in one root (pole) being real valued. The value of this root was  $-6.4 \times 10^6$ , which is equivalent to minus the value of  $\frac{1}{d}$ . In this case variables a, b, c and d correspond to:

$$a = 2C_1C_2Req^2$$

$$b = 2Req((C_1 + C_2) - \frac{C_1C_2}{C_3}) \text{ or } (C_1 + C_2)Req$$

$$c = 2$$

$$d = \frac{C_3Req}{2}$$
(5.7)

$$2Req((C_1 + C_2) - \frac{C_1C_2}{C_3}) = (C_1 + C_2)Req$$

$$C_1 + C_2 - \frac{2C_1C_2}{C_3} = 0$$

$$C_3 = \frac{2C_1C_2}{C_1 + C_2}$$
(5.8)

The fragment representing  $2^{nd}$  order filter transfer, in equation (5.6), can now be rewritten to the standard formula [2]. Hence the transfer function will now resemble:

$$TF = Req \cdot \frac{\frac{1}{a}}{s^2 + \frac{b}{a}s + \frac{c}{a}} \cdot \frac{\frac{1}{d}}{s + \frac{1}{d}}$$

$$= Req \cdot \frac{\frac{1}{c}\omega_0^2}{s^2 + \frac{\omega_0}{Q}s + \omega_0^2} \cdot \frac{\frac{1}{d}}{s + \frac{1}{d}}$$
(5.9)

After filling in the value of  $C_3$  from equation (5.8) into the variables of equation (5.7) one can derive the Q-factor and the cut-off frequency of the filter:

$$a = 2C_1C_2Req^2$$

$$b = (C_1 + C_2)Req$$

$$c = 2$$

$$d = \frac{C_1C_2}{C_1 + C_2}Req$$
(5.10)

$$\omega_0^2 = \frac{c}{a} \Rightarrow \omega_0 = \sqrt{\frac{c}{a}} = \frac{1}{\sqrt{C_1 C_2 Req}}$$
 (5.11)

$$f_{cut-off} = \frac{1}{2\pi\sqrt{C_1C_2}Req} \tag{5.12}$$

$$\frac{1}{Q} = \frac{b}{a\omega_0}$$

$$\Rightarrow Q = \frac{a\omega_0}{b}$$

$$= \frac{\sqrt{ac}}{b}$$

$$= \frac{2\sqrt{C_1C_2}}{C_1+C_2}$$
(5.13)

According to the findings of Lulec, Johns and Liscidini [3] the definitions for the  $\omega_0$  and Q-factor of a  $2^{nd}$  order low-pass passive complex-pole switched-capacitor filter should be

$$\omega_0 = \frac{\sqrt{2}}{\sqrt{C_1 C_2 Req}}$$
 and  $Q = \frac{\sqrt{2C_1 C_2}}{C_1 + C_2}$  (5.14)

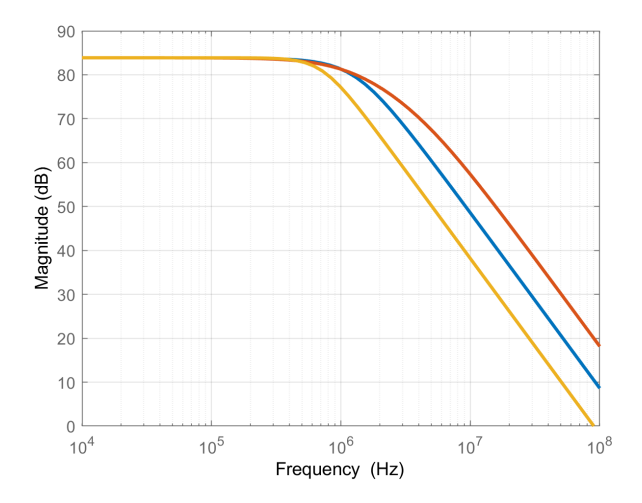
This is in agreement with the results obtained in equation (5.3) and (5.5). Furthermore, from equation (5.5) and (5.13) one can conclude that the Q-factor is independent of the sampling frequency and the value of the sampling capacitor  $(C_S)$ , while there is no  $Req(=\frac{1}{f_sC_S})$  term in the Q-factor equation. For this reason one can choose an appropriate value for  $C_S$ . In this case a choice was made to set the value to 200fF. However, the cut-off frequency (equation 5.4 and 5.12) does depend on Req, which implies that one can reconfigure the bandwidth (frequencies until cut-off frequency) of the filter by changing the capacitor ratio  $(\frac{C_1}{C_2})$  and the sampling frequency (switch clock). Moreover, when comparing the final results of equation (5.5) with (5.13) one could assume that there is a relation between the  $2^{nd}$  and  $3^{rd}$  order filter Q-factor. The  $3^{rd}$  order filter Q-factor could be obtained from the Q-factor of the  $2^{nd}$  order multiplied by  $\sqrt{2}$ . This could imply that the Q-factor of any arbitrary order higher than two can be determined from the Q-factor of one order lower.

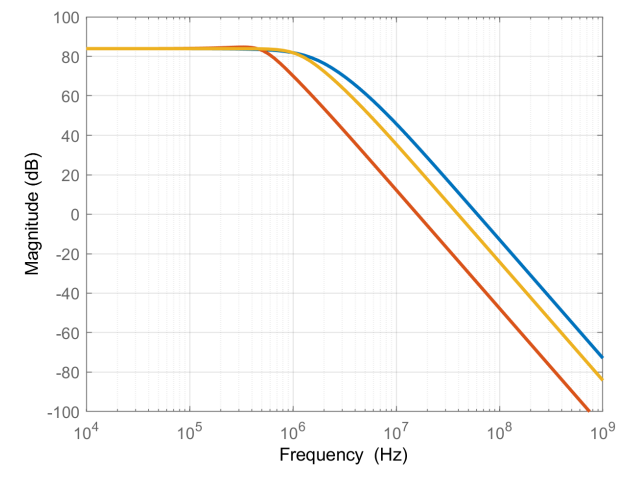
### 5.2 Influence of Q-factor on the Magnitude Behaviour of a Filter.

According to figure 5.1 and 5.2 the rate by which the filter rolls off is dependent on the value of the Q-factor. Both figures indicate that this roll-off rate  $^1$  increases when the Q-factor rises. This is caused by the transition between filter states when the Q-factor is increased. In case of the presented figures, the filters then change from being in a critically damped  $(Q = \frac{1}{2})$  to an under damped  $(Q > \frac{1}{2})$  state or from an under damped to even more under damped state [13]  $^2$ . When a filter becomes under damped the frequency response around the cut-off frequency will display a sharper "peaking" behaviour and a faster roll-off rate [14].

<sup>&</sup>lt;sup>1</sup>Transition between in band and out of band

 $<sup>^2</sup>$  [13] describes the conditions for a critically and under damped system in terms of relative damping  $\zeta$ , the Q-factor conditions can be derived by  $Q=\frac{1}{2\zeta}$ 



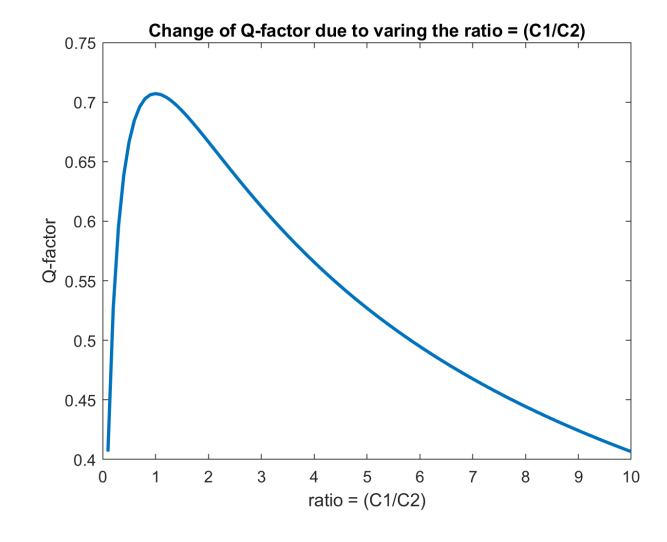


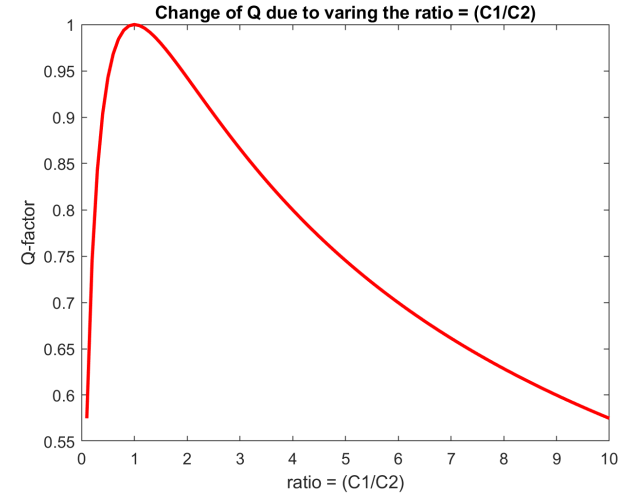
**Figure 5.1:** Magnitude plot of the  $2^{nd}$  order filter Transfer Function for Q-factor values of 0,4066 (Red), 0,5958 (Blue) and 0,7071 (Yellow)

Figure 5.2: Magnitude plot of the  $3^{rd}$  order filter Transfer Function for Q-factor values of 0,5750 (Blue), 0,7454 (Yellow) and 1 (Red)

### 5.3 Q-factor maximization vs Capacitance-ratio

Figure 5.3 and 5.4 show the relation between the Q-factor and the capacitor  $\operatorname{ratio}(\frac{C_1}{C_2})$ . This ratio was derived from the Q-factor equations (5.5) and (5.13). There was brought to light that the Q-factor for the  $2^{nd}$  and  $3^{rd}$  order low-pass passive complex-pole switched-capacitor filter depends on the values of  $C_1$  and  $C_2$ . Both figures show that the maximum Q-factor is achieved when the ratio equals 1. The maximum Q-factor for the  $2^{nd}$  order filter is 0,7071 and for the  $3^{rd}$  order is 1.





**Figure 5.3:**  $2^{nd}$  order filter - Q-factor vs ratio

**Figure 5.4:**  $3^{rd}$  order filter - Q-factor vs ratio

# 5.4 Comparison between the simulations based on calculated transfer function and the Adjoint Network approach for maximum achieved Q-factor

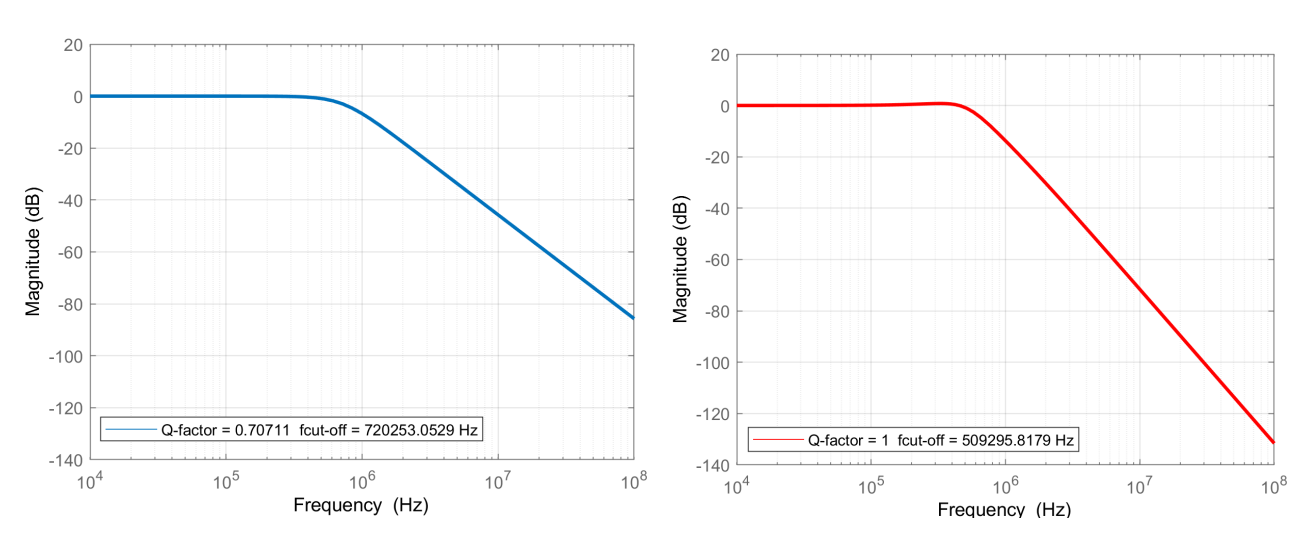


**Figure 5.5:** Magnitude plot  $2^{nd}$  order by Matlab simulation

**Figure 5.6:** Magnitude plot  $3^{rd}$  order by Matlab simulation

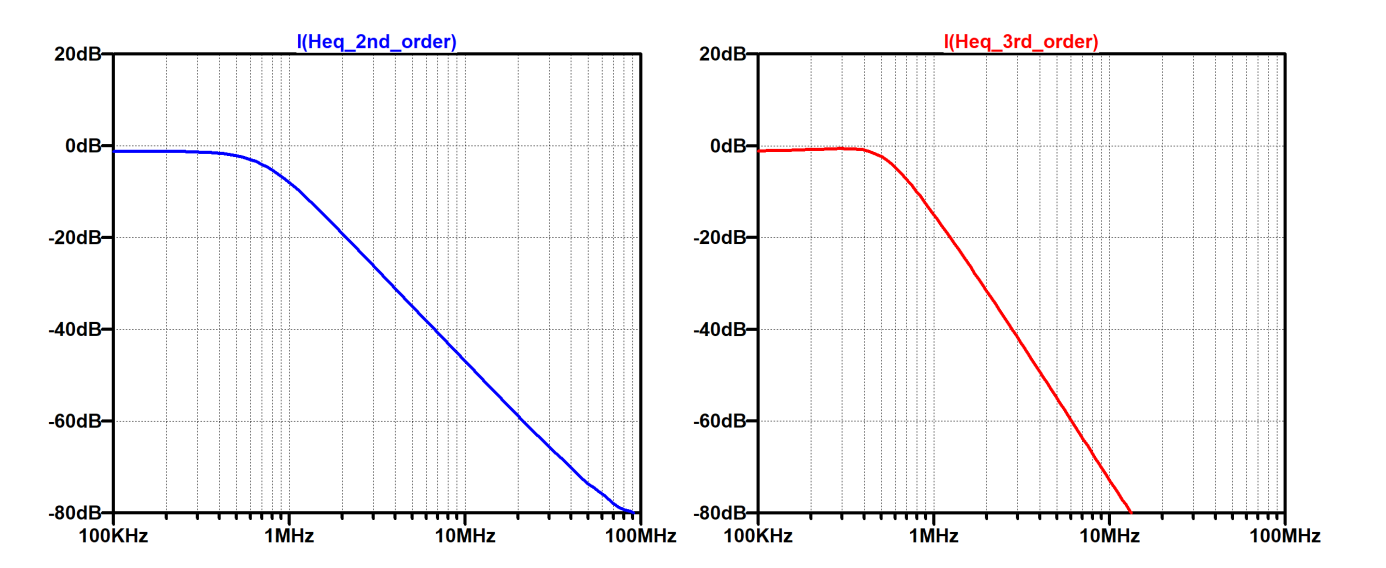


**Figure 5.7:** Magnitude plot  $2^{nd}$  order by LTspice simulation

**Figure 5.8:** Magnitude plot  $3^{rd}$  order by LTspice simulation

Figure 5.5 until 5.8 display the normalized<sup>3</sup> magnitude response for the  $2^{nd}$  and  $3^{rd}$  order low-pass passive complex-pole switched-capacitor filter at maximum Q-factor (see previous section). However, the results in figure 5.5 and 5.6 were obtained from calculations and

 $<sup>^3</sup>$ All figures were normalized in such a way that the starting magnitude equaled 0dB. For figure 5.5 and 5.6 this was achieved by dividing out the DC gain terms in their transfer functions. In case of figure 5.7 and 5.8, the  $g_m$  values of the transconductors (figure 4.3 and 4.4) were set to 1kS

those of figure 5.7 and 5.8 using the method described in chapter 4. As can be seen the calculated cut-off frequencies in figure 5.5 and 5.6 were 720kHz and 509kHz. While the ones in figure 5.7 and 5.8 equal 717kHz and 586kHz. When a comparison is made between the results obtained by calculation and those by LTspice simulation one can concluded:

- Figure 5.5 and 5.7 display an stopband attenuation of 40dB/decade.
- Figure 5.6 and 5.8 display an stopband attenuation of 60dB/decade.
- The cut-off frequency difference between the calculations and simulation is 3kHz (decrease of 0,4%) for the  $2^{nd}$  order filter and 77kHz (increase of 15%) for the  $3^{rd}$  order. This implies that the calculation error for the  $3^{rd}$  order filter is greater than the one for the  $2^{nd}$  order.

## Conclusions and recommendations

#### 6.1 Conclusions

In this thesis a complete transfer function (TF) analysis is given for the  $2^{nd}$  and  $3^{rd}$  order low-pass passive complex-pole switched-capacitor filter. The transfer functions were determined using the simplified continuous time model for a passive complex-pole switched-capacitor filter and verified by LTspice simulations based on the "Adjoint Network" approach. Based on TF calculation simulations it can be concluded that the achievable Q-factor is limited to a maximum value. For the  $2^{nd}$  order filter this value equals 0,7071 and in case of the  $3^{rd}$  order 1. The bandwidth of both filters can be reconfigured by changing the capacitor ratios and the sampling frequency.

Furthermore, the filter roll-off rate increases with the increase of the Q-factor. According to the compression between the results obtained from TF calculation and LTspice simulations, one can deduce that both simulations show the same stopband attenuation for a specific filter. Moreover, there is an increase in error between both simulation types. Looking at the  $2^{nd}$  order filter simulations this error amounts to 0,4% and for the  $3^{rd}$  order it equals 15%.

#### 6.2 Recommendations

This thesis was limited to the evaluation of low-pass passive complex-pole switched-capacitor filters of the  $2^{nd}$  and  $3^{rd}$  order. A recommendation would be to investigate higher order filters of this kind with the purpose of evaluating if a general relation between the Q-factors of different filter orders can be derived and to verify if the difference in cut-off frequency for a specific filter increases with the order. Moreover, it would be beneficial for future development to check if other types of passive switched-capacitor filters can be developed using the presented simplified model. For example high-pass, bandpass, all-pass or notch filters.

## **Bibliography**

- [1] Z. Sohrabi and A. Jannesari, "Analysis and design of discrete-time charge domain filters with complex conjugate poles," *INTERNATIONAL JOURNAL OF CIRCUIT THEORY AND APPLICA-TIONS*, vol. 45, no. 4, pp. 530–549, 2017.
- [2] K. Lacanette, "A Basic Introduction to filters-active, Passive and Switched-Capacitor," 21 April 2010. [Online]. Available: "http://www.ti.com/lit/an/snoa224a/snoa224a.pdf"
- [3] S. Z. Lulec, D. A. Johns, and A. Liscidini, "A Simplified Model for Passive-Switched-Capacitor Filters With Complex Poles," *IEEE TRANSACTIONS ON CIRCUITS AND SYSTEMS—II: EXPRESS BRIEFS*, vol. 63, no. 6, pp. 513–517, June 2016.
- [4] K. R. Tony, "Capacitor Quirks Chapter 4 Reactance And Impedance Capacitive," 2019. [Online]. Available: "https://www.allaboutcircuits.com/textbook/alternating-current/chpt-4/capacitor-quirks/"
- [5] M. Tohidian, I. Madadi, and R. B. Staszewski, "Analysis and Design of a High-Order Discrete-Time Passive IIR Low-Pass Filter," *IEEE JOURNAL OF SOLID-STATE CIRCUITS*, vol. 49, no. 11, pp. 1–13, November 2014.
- [6] S. Z. Lulec, D. A. Johns, and A. Liscidini, "A 150-W 3rd-Order Butterworth Passive-Switched-Capacitor Filter with 92 dB SFDR," *2017 Symposium on VLSI Circuits*, pp. 142–143, 2017.
- [7] M. Bentum, J. Eikel, F. van der Heijden, M. Odijk, C. Salm, and L. Segerink, *Introduction to electrical engineering and electronics*. University of Twente, 2016, pp. 75–94.
- [8] N. Davis, "An Introduction to Filters," 31 July 2017. [Online]. Available: "https://www.allaboutcircuits.com/technical-articles/an-introduction-to-filters/"
- [9] A. J. Annema, *Module 3: Electronics*. University of Twente, 2016, pp. 37–28.
- [10] J. W. Nilsson and S. A. Riedel, *Electric Circuits*, 10th ed. Harlow: Pearson Eductation Limited, 2015, pp. 769–771.
- [11] A. J. Annema, Module 3: Electronics. University of Twente, 2016, pp. 139-146.
- [12] S. Pavan and E. Klumperink, "Simplified Unified Analysis of Switched-RC Passive Mixers, Samplers, and N-Path Filters Using the Adjoint Network," *IEEE TRANSACTIONS ON CIRCUITS AND SYSTEMS—I: REGULAR PAPERS.*, vol. 64, no. 10, pp. 2714–2725, October 2017.
- [13] P. Breedveld, *Integrated Modeling of Physical Systems*. University of Twente, 2016, pp. 1.139–1.140
- [14] "Second Order Filters," 2019. [Online]. Available: "https://www.electronics-tutorials.ws/filter/second-order-filters.html"

### **Appendix A**

## **Appendix**

## A.1 Code - $2^{nd}$ order lowpass Passive Complex-Pole Switched-Capacitor Filter

```
1 clc
2 close(gcf)
3 %Parameters
4 q=0;
5 fs=160e6;
6 Cs = 200e - 15;
7 factor=(0.1:0.1:10); % creating a array of factors C1/C2, !!!!!remember to
      change the range before making figure (2)
8 C2=10e-12;
9 C1=factor*C2;
10 lengthC1=length(C1); % max length of the array of c1 values
natrix_of_factor_Q_f0_Poles=ones(lengthC1,5);
12 Req=1/(fs*Cs);
14 for i=1:lengthC1% this for-loop changes the C1 values one by one
15 %Formulae
16 H0 = (Req)/2;
17 W02 = (2/(C1(i)*C2*(Req^2)));
18 W0=sqrt(W02);
19 f0=W0/(2*pi);
20 Q=1/((C1(i)+C2)/(sqrt(2*C1(i)*C2)));
21 %TF definition
22 N=[W02]; % numerator of the TF
23 D=[1 (W0/Q) W02];%denominator of the TF
24 TF_sub=tf(N,D);%sub component of the TF
25 TF=H0*TF_sub;%TF % For normalization delete H0 term
26 %Generation of a matrix with all values of the factor with the belonging
27 %values of Q and fO an a pole matrix
28 matrix_of_factor_Q_f0_Poles(i,1)=factor(i);
29 matrix_of_factor_Q_f0_Poles(i,2)=Q;
30 matrix_of_factor_Q_f0_Poles(i,3)=f0;
31 matrix_of_factor_Q_f0_Poles(i,4:5)=roots(D);
32 %Max Q with the belonging TF and f0
33 if (Q>q)
      Q_MAX=Q;
```

```
35
      q = Q;
      TF_at_Q_MAX = TF;
36
      fO_at_Q_MAX = fO;
      WO_at_Q_MAX = WO;
39 else
40
      Q_MAX=q;
41 end
      Q = Q _MAX;
43 %Plot of the influence of different Q, comment out figure (2) when running
      code for a long range of values of C1
44 % figure(2)
45 % opts=bodeoptions('cstprefs'); % Initialization of Bode plot options.
46 % opts.PhaseVisible='off'; % Displaying Phase plot. Commands 'on'/'off'.
47 \% opts.Title.String='Magnitude plot of a 2nd order Switched-Capacitor Filter
      for different Q-factors'; %Change lable of specific text => title.
48 % opts.FreqUnits='Hz'; %Specifying frequency axis units.
49 % opts.Grid='on'; %Show/hide grid=> 'on'/'off'.
50 % hold on
51 \% bodeplot(TF,opts)\% Initialization command to make a bode plot with grid.
52 % hold off
53 % legend(strcat('Q=',num2str(matrix_of_factor_Q_f0_Poles(:,2))))%,'Location
      ','BestOutside','Orientation','vertical')% Creating a legend.Always keep a
       space between the variable that you want to display and its readout
      num2str()
54 end
55 %Plot of the TF with the highest Q factor
56 figure (3)
57 opts=bodeoptions('cstprefs'); %Initialization of Bode plot options.
58 %opts.Ylim=[-140,20]; % decomment for normalization to change y-axis limits
59 opts.PhaseVisible='off'; % Displaying Phase plot. Commands 'on'/'off'.
60 opts.Title.String='Magnitude plot at maximum Q-factor'; %Change label of
      specific text => title.
opts.FreqUnits='Hz'; %Specifying frequency axis units.
62 opts.Grid='on';%Show/hide grid=> 'on'/'off'.
64 bodeplot(TF_at_Q_MAX,opts)% Initialization command to make a bode plot with
65 set(findall(gcf,'type','line'),'linewidth',2)
66 hold off
67 legend(['Q-factor = ' num2str(Q_MAX), ' fcut-off = ' num2str(f0_at_Q_MAX) '
      Hz'],'Location','BestOutside','Orientation','vertical')% Creating a legend
      . Always keep a space between the variable that you want to display and its
      readout num2str()
68 %Plot of the Q vs factor = (C1/C2)
69 figure (4)
70 plot(matrix_of_factor_Q_f0_Poles(:,1),matrix_of_factor_Q_f0_Poles(:,2),'
      LineWidth',2.0)%Create plot of Q vs factor = (C1/C2)
71 title('Change of Q-factor due to varying the ratio = (C1/C2)')%Create title
72 xlabel('ratio = (C1/C2)')%Label x-axis
73 ylabel('Q-factor')%Label y-axis
```

## A.2 Code - $3^{rd}$ order lowpass Passive Complex-Pole Switched-Capacitor Filter

```
1 clc
2 close(gcf)
3 %Parameters
4 q = 0;
5 fs=160e6;
6 factor=(0.1:0.1:10); % creating a array of factors C1/C2, !!!!!remember to
      change the range before making figure (2)
7 C2=10e-12;
8 C1=factor*C2;
9 C3=(2*C1*C2)/(C1+C2);
10 Cs = 200e - 15;
11 lengthC=length(C1);% max length of the array of c1 values
12 matrix_of_factor_Q_f0_Poles=ones(lengthC,6);
original_pole_matrix=ones(lengthC,3);
14 Req=1/(fs*Cs);
15 for i=1:lengthC% this for-loop changes the C1 values one by one
16 %Formulae
17 a=2*C1(i)*C2*Req^2;
18 c=2;
19 d=(C3/2)*Req;
20 b=(C1(i)+C2)*Req;
21 H1=1/a;
122 H2=1/d;
23 H0=Req*H1*H2;
24 \text{ W}02=c/a;
25 W0=sqrt(W02);
26 f0=W0/(2*pi);
27 Q=(a*W0)/b;
28 %TFcheck definition
29 Nn=[Req]; % numerator of the TF
C2+C3)*Req) 2]; %Denominator of the TF
31 TFcheck=tf(Nn,Dd); %TF
32 poles=roots(Dd);
33 %TF definition
34 N=[Req]; % numerator of the TF %set to 2 for normalization
35 D=[(a*d) (a+b*d) (b+c*d) c]; %denominator of the TF
36 TF_sub=tf(N,D);%sub component of the TF
37 TF=TF_sub; %TF
38 %Generation of a matrix with all values of the factor with the belonging
39 %values of Q and fO an a pole matrix
40 matrix_of_factor_Q_f0_Poles(i,1)=factor(i);
41 matrix_of_factor_Q_f0_Poles(i,2)=Q;
42 matrix_of_factor_Q_f0_Poles(i,3)=f0;
43 matrix_of_factor_Q_f0_Poles(i,4:6) = roots(D);
44 original_pole_matrix(i,1:3)=roots(D);
45 %Max Q with the belonging TF and fO
```

```
46 if (Q>q)
      Q_MAX=Q;
      q = Q;
48
      TF_at_Q_MAX= TF;
      f0_at_Q_MAX = f0;
51 else
52
      Q_MAX=q;
53 end
      Q = Q _MAX;
55 %Plot of the influence of different Q, comment out figure(2) when running
      code for a long range of values of C1
56 % figure (2)
57 % opts=bodeoptions('cstprefs'); % Initialization of Bode plot options.
58 % opts.PhaseVisible='off'; % Displaying Phase plot. Commands 'on'/'off'.
59 % opts. Title. String='Bode plot of a 3rd order Switched-Capacitor Filter';%
      Change label of specific text => title.
60 % opts.FreqUnits='Hz'; %Specifying frequency axis units.
61 % opts.Grid='on';%Show/hide grid=> 'on'/'off'.
63 % bodeplot(TF,opts)% Initialization command to make a bode plot with grid.
64 % hold off
65 end
66 %Plot of the TF with the highest Q factor
67 figure (6)
68 opts=bodeoptions('cstprefs');%Initialization of Bode plot options.
69 opts.PhaseVisible='off'; % Displaying Phase plot. Commands 'on'/'off'.
70 opts.Title.String='Magnitude plot at maximum Q-factor'; %Change label of
      specific text => title.
71 opts.FreqUnits='Hz'; %Specifying frequency axis units.
72 opts.Grid='on';%Show/hide grid=> 'on'/'off'.
74 bodeplot(TF_at_Q_MAX,'r',opts)% Initialization command to make a bode plot
      with grid.
75 set(findall(gcf,'type','line'),'linewidth',2)
77 legend(['Q-factor = ' num2str(Q_MAX), ' fcut-off = ' num2str(f0_at_Q_MAX) '
      Hz'],'Location','BestOutside','Orientation','vertical')% Creating a legend
      . Always keep a space between the variable that you want to display and
      its readout num2str()
78 %Plot of the Q vs factor = (C1/C2)
79 figure (7)
80 plot(matrix_of_factor_Q_f0_Poles(:,1),matrix_of_factor_Q_f0_Poles(:,2),'r','
      linewidth',2)%Create plot of Q vs factor = (C1/C2)
81 title('Change of Q due to varying the ratio = (C1/C2)')%Create title
82 xlabel('ratio = (C1/C2)')%Label x-axis
83 ylabel('Q-factor')%Label y-axis
```